

## Two-dimensional unsteady problems of expansion of compressed gas volume(\*)

V.P. KOROBENIKOV, P.I. CHUSHKIN, L.V. SHURSHALOV (MOSCOW)

THE PAPER presents original, two-dimensional problems of unsteady expansion of a compressed gas volume into the surrounding compressible medium. Special attention is focused on the problem of expansion of a cylindrical gas volume, radius of the cylinder being finite, and its length—finite or semi-infinite. The considerations are mainly based on numerical calculations. Determined are the distributions of the disturbed flow parameters, propagation of the impact wave front, motion of the contact surface and formation of the secondary impact wave. Certain gas-dynamic effects are discussed. The solution concerning the expansion of a semi-infinite cylinder is used as a model of the problem of explosions of a falling meteoroid. Also considered are the two-dimensional, self-similar problems of evolution of arbitrary discontinuity in angular regions, including configurations with two or more states.

W pracy rozpatruje się nowe dwuwymiarowe zagadnienia nieustalonego procesu ekspansji sprężonej objętości gazu w otaczający tę objętość idealny ośrodek ściśliwy. Przede wszystkim rozważono przypadek ekspansji gazu zajmującego obszar walca o skończonym promieniu i skończonej bądź półnieskończonej długości. Rozważania oparte są w większości na analizie numerycznej. Określa się rozkład parametrów przepływu zaburzonego, przemieszczanie się frontu zaburzenia i powierzchni kontaktu oraz powstawanie fali uderzeniowej drugiego rzędu. Omówiono pewne zjawiska typu gazodynamicznego. Rozwiązanie zadania o ekspansji walca półnieskończonego wykorzystać można dla modelowania wybuchów spadającego meteorytu. Rozważono także dwuwymiarowe, samopodobne zagadnienia o dowolnej nieciągłości w obszarach kątowych uwzględniając konfiguracje z dwoma lub większą liczbą stanów.

Изучаются новые двумерные нестационарные задачи о разлете объема сжатого газа в окружающую сжимаемую идеальную среду. В основном рассматриваются случаи, когда разлетается цилиндрический объем конечного радиуса и конечной или полубесконечной длины. Большая часть исследования проводится с помощью численного анализа. Определяется распределение параметров возмущенного течения. Изучаются распространение ударного фронта, движение контактной поверхности и возникновение вторичной ударной волны. Выявлены некоторые газодинамические эффекты. Решение задачи о разлете полубесконечного цилиндра используется для моделирования взрыва летящего метеорита. Рассматриваются двумерные автомодельные задачи о распаде произвольного разрыва в угловых областях, включая конфигурации с двумя и большим числом состояний.

### 1. Introduction

TWO-DIMENSIONAL non-stationary problem involving expansion of a compressed gas contained in a volume of various shape belongs to the class of problems concerning decomposition of arbitrary discontinuity. They are useful for studying a number of theoretical and applied aspects in gas dynamics. In particular, the solutions of these problems can be used to simulate certain blast phenomena with instantaneous detonation of explosive charge or to treat non-one-dimensional gas flows in shock tubes.

(\*) Presented at 13th International Congress on Theoretical and Applied Mechanics, August 21–26, 1972, Moscow, U.S.S.R.

The basic problem under consideration is formulated as follows. A cylindrical volume with radius and length of finite sizes (in a special case, the length may be semi-infinite) is at rest in an unbounded medium. This volume is filled by a gas at the pressure which may be non-uniformly distributed and significantly exceeds the pressure in the external region. The ambient medium is assumed to be two-parametric ideal compressible — in a particular case, it can be considered as a perfect gas. At a certain moment of time, the gas contained inside the cylindrical volume begins to expand into the external space. The problem is to determine the motion of shock wave and contact surface bounding the expanding gas and to find the flow parameters in the entire region embraced by the shock front. The problem formulated is axisymmetrical and non-stationary. In the general case, this problem does not respond to an analytical approach and is studied by means of numerical analysis. The finite-difference method [1] is applied to the solution of the problem. In the greater part of the present paper, a numerical scheme is used in which the main shock wave and the contact surface are treated as lines of the network, all the necessary boundary conditions being exactly satisfied. In some cases (the calculations in Sec. 3 and the last example in Sec. 5), the shock wave and contact discontinuity are not treated explicitly, their locations being identified by taking into account gradients of gasdynamic functions. In the same manner are determined the locations of secondary shock waves arising in the disturbed flow region. The numerical solution enables study of the propagation of shock front and contact surface and the obtainment of gasdynamic parameter distributions at different times.

## 2. Expansion of a cylindrical gas volume with finite length

First, the solution of the problem concerning expansion of a cylindrical gas volume with finite length is investigated. The resulting flow is similar to the flow produced by an explosion of a cylindrical charge with finite length and radius. Some preliminary results of the solution were published in [2].

As an example, we shall analyse the case in which the cylinder radius/length ratio  $r_0/2l_0 = 0.05$ , the value of adiabatic exponent  $\gamma = 1.4$  for both gases and the ratio of pressure and density in the compressed gas to the corresponding quantities in the ambient medium are equal to  $10^4$  and  $10^2$ , respectively.

The successive positions of shock wave (solid line) and contact discontinuity (dashed line) are shown in Fig. 1 for several values of dimensionless time,  $\tau = t/t_0$ , where  $t_0 = l_0(\rho_1/p_1)^{1/2}$ ,  $p_1$  and  $\rho_1$  are pressure and density of ambient gas. In view of symmetry, it suffices to consider only one quadrant of the entire flow region. The region initially occupied by the compressed gas is shaded. The radial and axial coordinates are denoted by  $r$  and  $Z$ , respectively.

The shape and features of the moving shock wave depend on the form of cylindrical charge. The corner point at the cylinder end very essentially influences on the shock wave behaviour and the entire flow. The causes of this effect are as follows.

The shock wave at the moment of its formation is located in the immediate vicinity of the cylindrical volume, and in practice has the shape of this volume. The shock strength

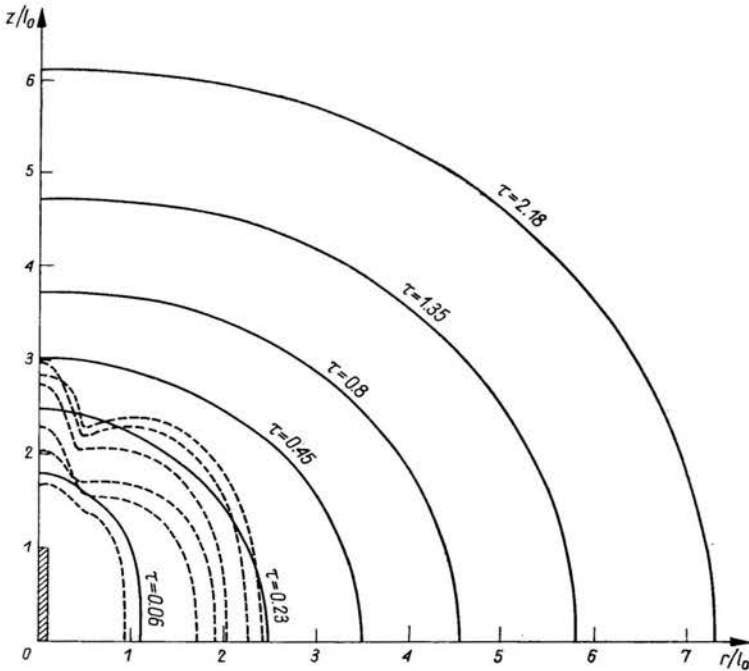


FIG. 1 Flow pattern for explosion of cylindrical charge with finite length.

is constant everywhere and it is equal to the strength resulting from the decomposition of the corresponding discontinuity on the interface between cylindrical gas volume and ambient medium. Then the shock strength decreases at different rates along different portions of the shock wave; therefore, the gasdynamic parameters change along the shock front. The flow character for short times  $\tau$  is locally plane at  $r = 0$ , locally cylindrical  $Z = 0$ , and qualitatively spherically-divergent at the corner point of the cylinder end. Accordingly, the shock strength decreases most rapidly in the vicinity of the corner point and most slowly at  $r = 0$ . As a result, initially the shock wave detachment distance is minimal near the corner point. For this reason, there occurs here a bend in the shock front. With increase of time, this bend gradually turns into an almost flat surface which then becomes convex.

For increasing time, the local properties of flow change. Qualitatively the flow near the charge end becomes entirely spherically-divergent, while a cylindrically divergent flow remains near the axis  $Z = 0$ . Hence, beginning from some sufficiently small  $\tau$ , the shock wave has maximal intensity at  $Z = 0$  and minimal intensity at  $\tau = 0$ , while along the front there takes place an almost monotonic change of parameters. Such a property is inherent for all moments of time presented in Fig. 1 and determines the dynamics of shock wave propagation at this stage. Here, the shock wave is stretched in the direction of the  $Z$ -axis. At  $\tau = 0.45$  it takes on a practically spherical form, but at longer time it is slightly extended along the  $r$ -axis. Beyond  $\tau > 1$ , the shape of the front approaches that of a sphere, the ratio of shock wave distances along  $r$  and  $z$  directions tends to one, though the difference between these distances continues to grow somewhat.

The behaviour of the contact surface is very interesting. There appears also a bend of this surface, which is due to the corner point of the cylinder end. The bend arises initially because of the non-uniformity of interface detachment distances and it becomes steeper with increasing  $\tau$ . The latter fact is connected with the effect of a secondary shock wave that occurs in a region engulfed by the contact surface and affects such surface. The secondary shock wave forming not far from the interface propagates into the central part of flow and gradually increases in strength. Crossing the secondary wave, the divergent gas stream slows down.

It is known from experiments and solutions of one-dimensional problems concerning expansion of compressed gas volumes that in spherical and cylindrical cases a secondary shock wave is observed. The formation of such a wave proceeds most intensively in the spherical case; therefore, in the flow under consideration the secondary shock wave arises first and is strongest in the region located opposite the corner point of the cylinder end. As a result, the corresponding portion of contact discontinuity, moving together with gas particles, slows down more than the other portions. This effect causes the increase referred to in the bend of the contact surface.

The velocity field for  $\tau = 0.23$  is shown in Fig. 2. Here the main shock wave, the contact surface and the secondary shock wave are represented by solid, dashed and dash-dotted

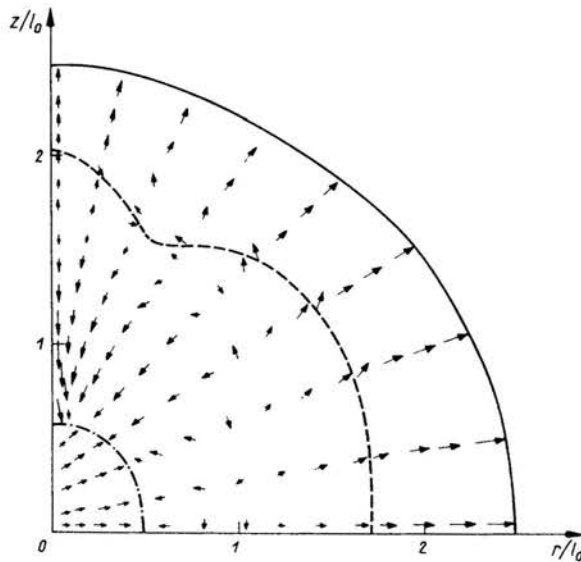


FIG. 2. Flow field for explosion of cylindrical charge with finite length.

lines, respectively. The arrows indicate velocity directions and their lengths are proportional to velocity magnitudes. The secondary wave strength is so large in this case that the flow is reversed. To be observed is even non-simultaneous stopping of some sections of the interface surface. After the reflection of a secondary shock wave in a central region, the gas engulfed by the contact surface again begins to expand and hence this surface continues a divergent motion.

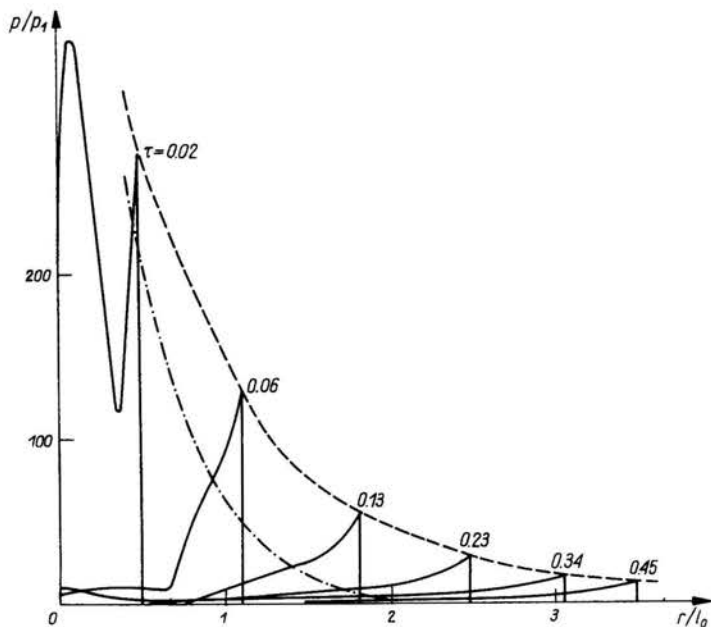


FIG. 3. Pressure distribution ( $Z = 0$ ) for explosion of cylindrical charge with finite length.

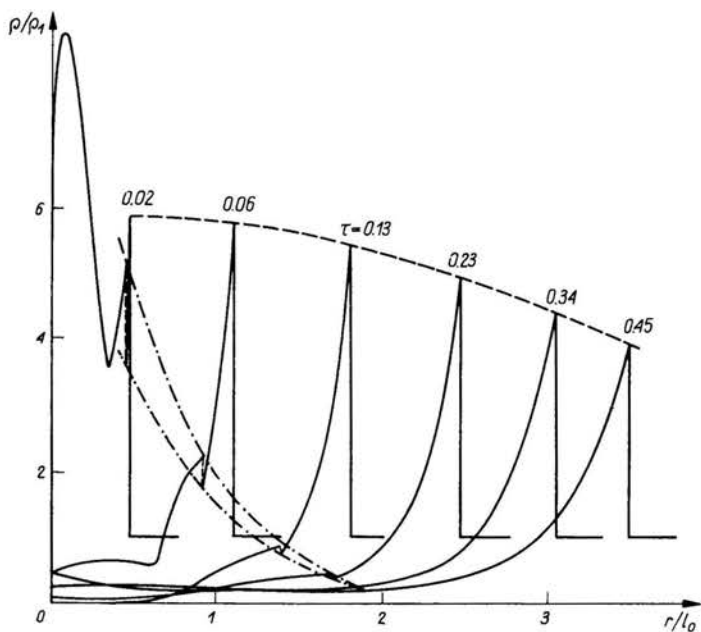


FIG. 4. Density distribution ( $Z = 0$ ) for explosion of cylindrical charge with finite length.

The distributions of relative pressure  $p/p_1$  and density  $\rho/\rho_1$  in the flow region are plotted in Figs. 3 and 4 by solid lines for a number of  $\tau$  at  $Z = 0$ . Here, the values on the shock front and the contact surface are represented by dashed and dash-dotted lines, respectively. In Fig. 4, the values of density ahead of behind the contact discontinuity are marked by the lower and the upper dash-dotted lines.

### 3. Expansion of semi-infinite cylindrical volume

Now, we shall consider the problem of expansion of a semi-infinite cylindrical volume of a compressed gas with uniform or non-uniform pressure and density distributions along the axis. This case corresponds to a model of blast of semi-infinite cylindrical charge with constant or variable specific explosion energy  $E_0$  along the axis.

Several types of specific energy distribution along the charge axis have been studied. In Fig. 5, uniform, exponential and step-like distributions are presented; in the last-named case, the specific energy in the head part of charge is ten times higher than in the tail part.

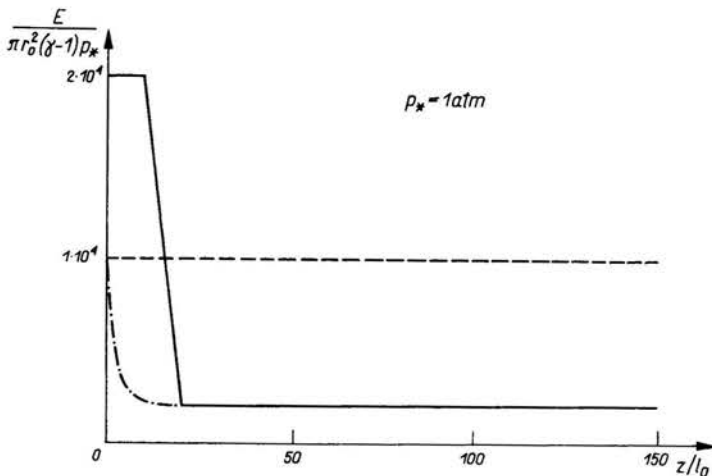


FIG. 5. Different variants of specific energy distribution along the axis of a semi-infinite cylindrical charge.

The shock wave shapes for a series of dimensionless times  $\tau = t/t_0$  [here  $t_0 = r_0(p_1/\rho_1)^{-1/2}$ ] in the cases of exponential and uniform energy distributions are shown in Figs. 6a and 6b, respectively. In the interests of symmetry, only the upper half of the flow pattern is given. The earlier stage of expansion is presented in Fig. 6a, where the region containing a compressed gas at  $\tau = 0$  is shaded. The energy in the head part of the charge does not greatly exceed the energy in the tail part, and for this reason the wave form at the later stage is similar to the wave form shown in Fig. 6a. At the earlier stage, the corner point at the cylinder end has a very marked influence on the shock front shape. As a result, an almost flat, long portion of the shock front occurs opposite this corner point. The shock wave in the case of uniform energy distribution represents a hemisphere-cylinder configuration (Fig. 6b). On moving from the cylindrical tail part to the hemispherical

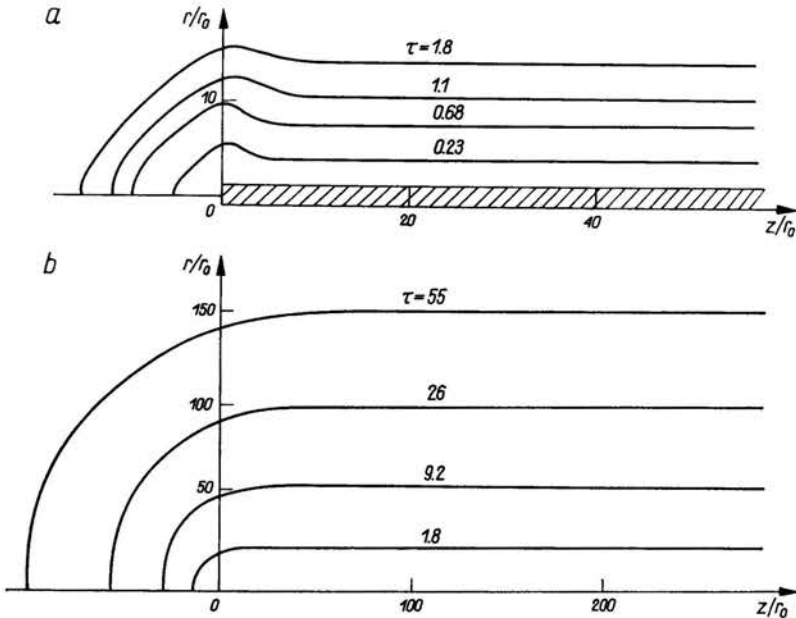


FIG. 6. Shape of shock wave for explosion of a semi-infinite cylindrical charge for two specific energy distributions along the axis.

head part, the strength of the shock wave decreases monotonically except for a short initial period when the effect of the corner point is important.

In the case of step-like energy distribution at  $\tau \geq 4.5$ , the shock wave also has the form of hemisphere-cylinder combination with an intermediate zone (see [3, 4]). The head part of shock wave at shorter  $\tau$  differs from a hemisphere because of influence of the corner point of the charge. There exists an effect of increasing wave strength in the intermediate zone between the hemispherical and cylindrical parts of shock front. The same is also found in the case of exponential energy distribution (Fig. 6a).

To determine the shock wave parameters at great distances, an approximate analytical approach was worked out [4]. Here, we apply the sector approximation in which the shock front is represented by a hemisphere-cylinder combination with an intermediate zone, where the shape and parameters of the shock wave are found by means of interpolation formulae.

#### 4. Application to the problem of explosion of a flying meteorite

The solution of the problem of expansion of semi-infinite cylindrical volume was applied to simulate a shock wave system arising for the flight and blast of large meteorite bodies in the Earth's atmosphere [3, 4]. Here, it is necessary to assume parameters characterizing the semi-infinite cylindrical charge and its position. The direction of the charge axis and the altitude of its head point above the ground are taken according to the meteorite trajectory before the blast. As regards the specific energy distribution along the

charge axis, it is possible to estimate this only with some degree of accuracy using, for example, the well-known hypersonic non-stationary analogy or some recorded consequences of explosion (seismograms, barograms, ground destructions).

The calculation of such a model cylindrical explosion, taking into account the non-homogeneity of the atmosphere and the wave reflection from the ground represents, an unsteady three-dimensional problem. For solving it, a method was developed based on a combination of numerical and analytical approaches [3, 4]. Note that there are three principal stages of this method. Firstly, the explosion is computed without taking into account the nonhomogeneity of the atmosphere and the wave reflection from the ground; here, at sufficiently strong shock wave is used the numerical solution and at later times the sector approximation. Secondly, allowance is made for the variation of atmospheric density using the quasi-one-dimensional ray theory and the hypothesis of plane sections. Thirdly, the initial stage of shock wave reflection from the Earth's surface is calculated; here, exact formulae [7] are considered in the case of regular reflection, while in the case of irregular reflection the results of [8] are used, where the graphs of overpressures behind a reflected wave are given in dependence on inclination angles and overpressures for an incident wave.

The extension and character of ground destructions are determined by static and dynamic pressures behind a shock wave reflected from the Earth's surface. If there is a forest in the place of explosion, it may be flattened, as happened in the case of the impact and blast of the Tunguska cosmic body. Some calculated patterns of forest flattening for the model meteorite explosion are given in Fig. 7. Here, the influence of the meteorite trajectory gradient upon the shape inextension of ground destruction zone is analysed. The following parameters of model blast are assumed: the altitude of the head point of the charge above the Earth,  $H_0 = 5$  km; total energy of the explosion wave in the head part of the cylindrical charge  $E_{ew} = 5 \cdot 10^{22}$  erg; the specific energy in the tail part of the charge, corresponding to the energy of a ballistic wave,  $E_{bw} = 4 \cdot 10^{15}$  erg/cm. Three values of inclination angle charge axis (i.e. inclination angle of the trajectory) are considered — namely,  $\alpha = 20^\circ, 40^\circ$ .

In Fig. 7, the solid lines are the contour lines of equal dynamic pressure behind the reflected wave, corresponding to  $\rho v^2 = 0.008$  kg/cm<sup>2</sup> ( $\rho$  — the density of air,  $v$  — the horizontal velocity component). According to the data [9], such a dynamic pressure knocks down about 5 per cent of trees. The dashed lines are isochrones (i.e. lines of equal moment of arrival of the shock wave on the ground); the arrows indicate the directions of trees overturning. The boundary between the zones of regular (situated on the right) and irregular (situated on the left) reflection of the shock wave is represented by the dash-dotted line. It will be seen that the configuration of a flattened forest resembles a butterfly. The decrease of  $\alpha$  causes a considerable stretching of the wings of this butterfly and the formation of a deepening between them. The direction of trees overturning essentially depends on the angle  $\alpha$ . For  $\alpha = 40^\circ$ , these directions are practically radial, while for smaller angles  $\alpha$  deviations from the radial direction occur in the region of the butterfly wings. Varying the angle  $\alpha$  and other parameters of the model explosion, and making the corresponding computations, it is possible to obtain a pattern of forest flattening close to the picture actually observed at the site of the Tunguska catastrophe.



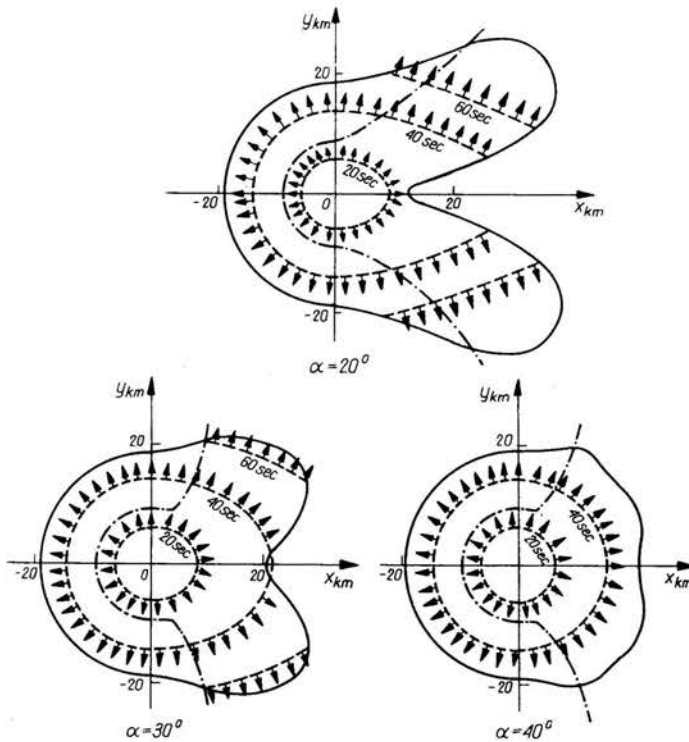


FIG. 7. Calculated patterns of forest flattening on the Earth by explosion of a flying meteorite.

## 5. Expansion of angle regions

Discussing the above problems, we have noted some flow features caused by the influence of the corner point at the end of cylindrical charge. In this connection, let us undertake a more detailed analysis of flow in the neighbourhood of the corner point of an expanding gas volume. We shall consider the two-dimensional self-similar problem concerning decomposition of an arbitrary discontinuity in angle regions filled with a compressed ideal gas. This problem has independent significance also. In [10] it was investigated analytically in linearized formulation only for the particular case of plane region with semiangle  $\beta$  close to  $\pi/2$ . In the present paper the numerical solution of this problem is given in the general case. The present method is applied both to plane and to conical angle regions. The calculations are carried out in physical variables  $x, y, t$  and then the results obtained are transformed into self-similar variables. As a result of the use of the finite-difference method, the numerical solution reaches the self-similar state not immediately but after some finite interval of time.

Now, we shall analyse the results of several calculations for plane angle regions. The main boundaries in the flow field (Fig. 8) are shown in the plane of self-similar variables  $\bar{x} = x/At$  and  $\bar{y} = y/At$ , where  $A = (p_1/\rho_1)^{1/2}$ ;  $p_2, \rho_2, \gamma_2$  and  $p_1, \rho_1, \gamma_1$  are pressure, density and adiabatic exponent of compressed and ambient gases, respectively. In this

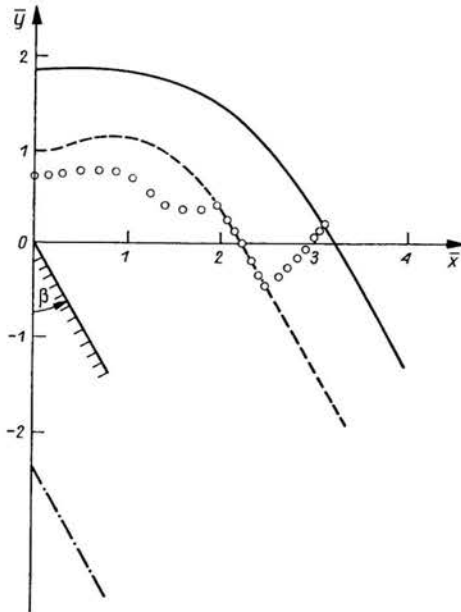


FIG. 8. Flow pattern for expansion of the angle region with semiangle  $\beta = 30^\circ$ .

case,  $\beta = 30^\circ$ ,  $p_2/p_1 = \rho_2/\rho_1 = 100$ ,  $\gamma_1 = \gamma_2 = 1.4$ . Here, the shock wave and the contact surface are depicted as solid line and a dashed line, respectively. The dash-dotted line corresponds to the head front of the expansion wave propagating in a compressed gas. The initial position of discontinuity is shown as a shaded line. The governing differential equations in self-similar variables are of mixed type. In Fig. 8, the position of the transition line (i.e., the boundary between the elliptical and hyperbolic regions) is plotted by circles, the elliptical zone being placed above this line. Crossing the interface, the transition line naturally has a break. The contact surface at  $\bar{x} = 0$  (opposite the apex of the angle) has a bend due to the influence of the secondary shock wave. The shock front has an almost plane long section near the  $\bar{y}$ -axis.

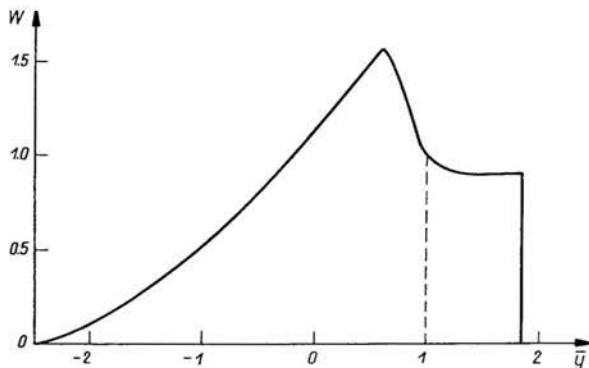


FIG. 9. Velocity distribution ( $\bar{x} = 0$ ) for expansion of the angle region with semiangle  $\beta = 30^\circ$ .

The distribution of the dimensionless vertical velocity component  $W = w/A$  along the  $\bar{y}$ -axis is plotted in Fig. 9. The dashed straight line marks the location of the contact surface. A sharp decrease of velocity occurs in the expanding gas region before this surface. This is connected with the passing of the secondary shock by gas particles. Since the secondary shock is not explicitly treated in the calculation, its front is manifested as a zone with large gradients. When a finer network is used, the width of this zone is reduced. The pressure and density distributions at  $\bar{x} = 0$  also maintain the presence of secondary shock at the same point. The intensity of the secondary shock wave drops rapidly when moving of the  $\bar{y}$ -axis. The position of this wave approximately coincides with the portion of the transition line below the contact surface (Fig. 8).

The flow features found in the case of  $\beta = 30^\circ$  are the same for other values of angle  $\beta < \pi/2$ , while a quite different flow pattern takes place for  $\beta > \pi/2$ . In Fig. 10, the

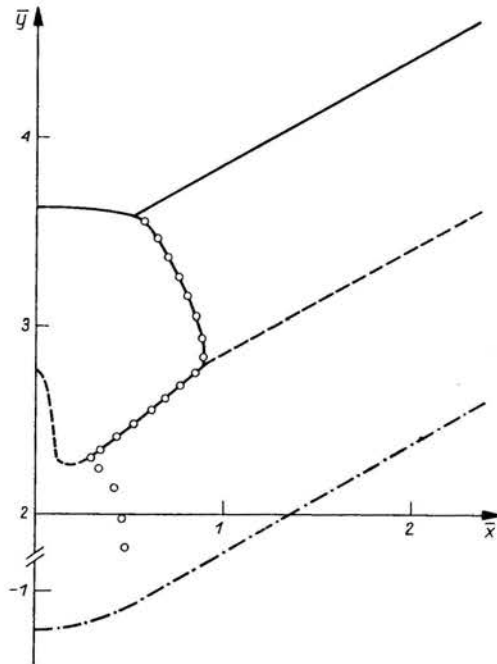


FIG. 10. Flow pattern for expansion of the angle region with semiangle  $\beta = 120^\circ$ .

configuration of main boundaries is shown in the case of  $\beta = 120^\circ$  and for the same values of other parameters as in Fig. 8. Again the solid, dashed and dash-dotted lines represent the shock wave, interface and head front of the expansion wave, respectively. The transition line is marked by circles, the elliptical zone being placed on the left near the  $\bar{y}$ -axis. The plane  $\bar{x} = 0$  may be regarded as a solid wall. It may be seen that from this wall there occurs irregular reflection of the incident shock wave. The position of the reflection wave coincides with the transition line in the region between the incident shock and the interface. The reflected wave is of weak intensity in the region of dense expanding gas (this part of the shock is not depicted in the figure). The behaviour of contact discon-

tinuity is highly interesting. Here is observed the formation of a cumulative jet. The presence or otherwise of this phenomenon depends essentially on the value of angle  $\beta$  (under the same other conditions). In particular, in the case of  $\beta = 150^\circ$  no cumulative jet arises, and the shock wave reflects from the plane  $\bar{x} = 0$  in a regular manner without the formation of any Mach stem.

The two-dimensional problem concerning decomposition of an arbitrary discontinuity can be generalized for the case with more than two angle regions. In this case, at the initial moment  $t = 0$ , a number of sectors containing gases with different states are considered. For  $t > 0$ , a complicated two-dimensional self-similar motion arises in the neighbourhood of the apex point, where the rays constituting the sector boundaries intersect. Without investigating in detail various cases which may take place here, we shall discuss one example with decomposition of triple configuration.

We consider three regions disposed of the initial moment of time  $t = 0$ , as is shown in the upper part of Fig. 11. They are marked by the numbers 1, 2, 3. A similar configura-

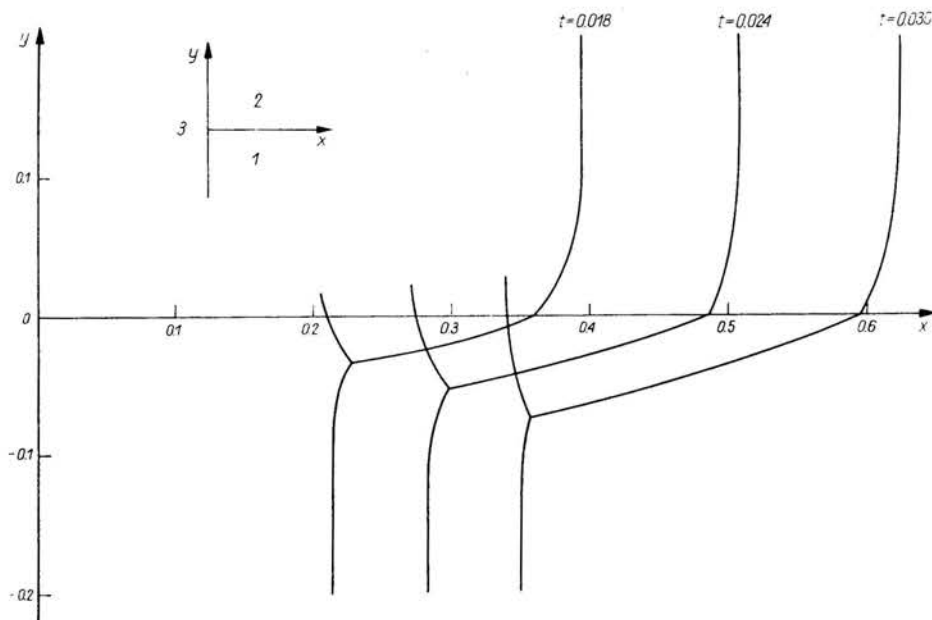


FIG. 11. Shock wave propagation for decomposition of triple configuration.

ration was calculated in [11] by means of Whitham's approximation [12]. The values of gas parameters in three regions are taken as follows:  $\gamma_1 = \gamma_2 = \gamma_3 = 7$ ,  $p_1 = p_2 = 1$ ,  $p_3 = 100$ ,  $\rho_1 = 1$ ,  $\rho_2 = 0.1$ ,  $\rho_3 = 2$  (pressure and density are referred to the corresponding values in region 1). In Fig. 11 is depicted the image of shock waves for three times in the physical variables  $x, y, t$  which are expressed in scaled units. It may be seen that the curves for different times are very similar to one another. Transformed into the self-similar variables  $x/t$  and  $y/t$ , they almost coincide, although there are certain distinctions connected with the different degree of approach to the limit self-similar solution.

Now let us discuss the dynamics of flow in this case. Since pressure in region 3 is higher than in regions 1 and 2, then the shock wave propagates in the last two regions. It moves faster in gas 2, having higher temperature and sound velocity than gas 1. Interacting with the interface surface, the forward moving wave weakens somewhat and transmits into gas 1, where its velocity decreases sharply. It meets at some point the shock wave propagating in gas 1. From this point, the third wave issues, which is the part of the main shock wave propagating in gas 1 and weakened due to the interaction with the interface and gas flow behind the wave transmitted from the region 2. The intensity of the third shock wave rapidly decreases with shifting of the intersection point of the three waves. The decomposition of triple configuration considered corresponds locally to the earlier stage of flow resulting from an explosion of a charge located on the interface between two media with different densities and partially submerged in both media.

The solutions obtained of several new two-dimensional non-stationary problems on expansion of different volumes of a compressed gas enable investigation of the corresponding flows with shock waves, and the indication of a number of interesting gasdynamic effects.

## References

1. С. К. Годунов, А. В. Забродин, Г. П. Прокопов, *Разностная схема для двумерных нестационарных задач газовой динамики и расчет обтекания с отошедшей ударной волной* [Finite difference scheme for two-dimensional, non-stationary problems of gasdynamics and calculations of flow with detached shock-waves, in Russian], Журнал вычислительной математики и математической физики, 1 6, 1020–1050, 1961.
2. Л. В. Шуршалов, *К расчету взрыва цилиндрических зарядов конечной длины* [On calculation of explosions of cylindrical charges of finite length, in Russian], Доклады Академии Наук СССР, 199, 6, 1262–1264, 1971.
3. V. P. KOROVENIKOV, P. I. CHUSHKIN, L. V. SHURSHALOV, *Gas dynamics of flight and explosion of meteorite bodies in the Earth's atmosphere*, Fluid Dynamics Transactions (eds. W. Fiszdon, Z. Płochocki, M. Bratos), 6, Part II, 351–359, PWN, Warszawa 1971.
4. V. P. KOROVENIKOV, P. I. CHUSHKIN, L. V. SHURSHALOV, *Gas dynamics of the flight and explosion of meteorites*, Astronautica Acta, 17, 339–348, 1972.
5. В. П. Коробейников, В. П. Карликов, *Определение формы и параметров фронта ударной волны при взрыве в неоднородной среде* [Determination of the shock-wave front parameters due to explosions in a non-homogeneous medium, in Russian], Доклады Академии Наук СССР, 148, 6, 1271–1274, 1963.
6. V. P. KOROVENIKOV, *Gas-dynamics of explosions*, Annual Review of Fluid Mechanics, 3, 317–346, 1971.
7. R. COURANT, K. FRIEDRICHS, *Supersonic flow and shock waves*, Interscience Publishers, New York 1948.
8. H. L. BRODE, *Review of nuclear weapons effects*, Annual Review of Nuclear Science, 18, 153–202, 1968.
9. *The effects of nuclear weapons* (ed. S. Glasstone), Washington 1964.
10. В. М. Тешуков, *Автоподобная задача о распаде двумерного разрыва* [Self similar problem of two-dimensional shock-wave degeneration, in Russian], Прикладная механика и техническая физика, 2, 29–38, 1972.
11. R. COLLINS, H.-T. CHEN, *Propagation of a shock wave of arbitrary strength in two half-planes containing a free surface*, Труды секции по численным методам в газовой динамике II Международного

коллеквиума по газодинамике взрыва и реагирующих систем (Новосибирск, 19–23 августа 1969), 1, 178–226, ВЦ АН СССР, Москва 1971.

12. G. B. WHITHAM, *On the propagation of shock waves through regions of non-uniform area of flow*, Journal of Fluid Mechanics, 4, 337–360. 1958.

COMPUTING CENTER  
ACADEMIE SCIENCES OF THE U. S. S. R., MOSCOW.

*Received May 3, 1973.*